Meteoritics 24, 35–42 (1989)

Isolated olivines in the Yamato 82042 CM2 chondrite: The tracing of major condensation events in the solar nebula

G. KURAT,[1] M. MAYR,[2] TH. NTAFLOS[1] AND A. L. GRAHAM[3]

[1]Naturhistorisches Museum, Postfach 417, A-1014 Wien, Austria
[2]VOEST-ALPINE AG, Postfach 2, A-4010 Linz, Austria
[3]British Museum (Natural History), Cromwell Road, London SW7 5BD, UK

(*Received 2 May 1988; accepted in revised form 27 February 1989*)

Abstract—Yamato 82042 is an unusual CM2 chondrite consisting mainly of phyllosilicates, a few olivines and carbonates, very minor sulphides and trace metal. Olivine occurs: (1) as isolated grains dispersed in the phyllosilicate matrix, (2) as constituents of mineral aggregates or accretionary fragments associated with abundant phyllosilicates and minor sulphides, and (3) as objects which resemble barred olivine chondrules also associated with phyllosilicates. Olivine, from all occurrences, ranges in composition from 0.26 to 22.6 weight % FeO, but generally contains less than 1.25 wt.% FeO. Minor element contents, particularly Ca, Al, and Cr, are relatively high and are generally correlated, as reported for olivines in other carbonaceous chondrites. However, we report here uncorrected trends for the same minor elements which occur in distinct areas (volumes) within the same olivines. These compositional trends may be due to condensation of olivine from a vapor of non-solar composition and partial mobilization of Ca during later annealing. If this is the case, the data may be used to trace changes in the Ca/Al ratio of the parent medium during the formation of these olivines, provided that it is possible to distinguish the effects of any post-formation annealing which could have redistributed the minor elements. Some isolated olivines show distinctive minor element zoning which severely limits the possibility of any post-formation redistribution of these elements. Accordingly, these isolated olivines indeed retain evidence of early condensation processes in the solar nebula, though non-classic conditions are implied for their formation.

INTRODUCTION

YAMATO 82042 (Y-82042) IS AN UNUSUAL carbonaceous chondrite; chemically it is a CM2 stone but with petrographic features which distinguish it from other CM2 stones (Grady *et al.*, 1986). The matrix consists of phyllosilicates within which are scattered rare grains of olivine, carbonates and very minor sulphides. Metal is very rare and exclusively occurs inside olivine grains. The olivines occur in three distinct modes: (1) as isolated grains dispersed within the phyllosilicate matrix, (2) as constituents of mineral aggregates or accretionary fragments together with abundant phyllosilicates and minor sulphides, (3) as objects which resemble barred olivine (BO) chondrules, associated with phyllosilicates. Compositionally, the olivines of Y-82042 define two populations, one FeO-poor (<1.25 wt.% FeO) and a second FeO-rich (>1.25 wt.% FeO); this is commonly the case with CM chondrites (see McSween, 1977 and references therein). The minor element contents of olivines in carbonaceous chondrites are generally higher than those of the olivines in non-carbonaceous chondrites (Hutchinson and Symes, 1972; Hoinkes and Kurat, 1975; Kurat, 1975; Kurat and Kracher, 1975; McSween, 1977; Desnoyers, 1980; Steele *et al.*, 1984, 1985a,b; Palme *et al.*, 1985, 1986; Skirius *et al.*, 1986; Steele, 1986a,b; Steele and Smith, 1986; Koeberl *et al.*, 1987; Kurat *et al.*, 1987). We report here the minor element contents (Ti, Cr, Al, Mn, Ca) of the FeO-poor olivines in Y-82042. Generally the correlations shown by these elements in the olivines confirm the previous work quoted above. However there are also indications of other inter-element variations that suggest that some olivines were not produced in a simple, single-stage process. A more complicated genetic model than previously suggested may be needed to explain their formation.

ANALYTICAL METHODS

The data were obtained using an ARL-SEMQ electron microprobe under conventional quantitative analytical conditions for silicates. Concentration maps were obtained using a computer-controlled stage movement and an individual spot count time of one second. The number of analyses made on each olivine crystal to produce the element concentration maps was of the order of three thousand, with the actual number depending on crystal size. These data were corrected for background, deadtime, drift and matrix effects using the Bence-Albee procedure. For concentration mapping the major matrix elements were not analysed, but a constant matrix composition of MgO = 57.0%, SiO_2 = 43.0% was used. The effect of the minor elements was neglected for this correction. The concentration mapping procedure has been described by Mayr and Angeli (1985).

RESULTS

The FeO content for Y-82042 olivines extends from 0.26 to 22.6 wt.%, with both extremes exclusively being present among the isolated olivines. The overwhelming majority of olivines from all occurrences has FeO <1.25 wt.% (Tables 1 and 2). All are rich in minor elements but with variable concentrations as shown in Fig. 1. This figure includes all data for olivines with less than 1.25 wt.% FeO which are from (1) olivine-phyllosilicate aggregates and (2) from isolated olivines. The concentrations of Mn and Ti were also measured but these elements are present at very low levels (<0.15% MnO, <0.08% TiO) and the quality of the data is too poor for these to be included in Fig. 1.

The ranges in the minor element contents are relatively large and within the range for "blue" olivines as reported by Steele (1986b): TiO_2 0–0.8%, Al_2O_3 0.03–0.25%, Cr_2O_3 0.06–0.63%, FeO 0.30–1.12%, MnO 0–0.14% and CaO 0.02–0.53%. The refractory elements Al and Ca and the moderately volatile elements Fe and Cr are generally well correlated, as has previously been described by Steele (1986a,b). However, the dominant correlation in the Al_2O_3-CaO diagram is good only for those olivines containing more than about 0.2% CaO. These are referred to as the high-Ca group and are distinct from those in the low-Ca group (CaO < 0.18%) which shows no correlation with Al_2O_3 content. The FeO-Cr_2O_3 plot shows a positive correlation (r = 0.802), but a few points are well off the correlation line at higher FeO contents. Figure 1 also shows negative correlations between elements that are refractory, *e.g.*, Ca and those

TABLE 1. Electron microprobe analyses of olivine from olivine-phyllosilicate aggregates and pseudochondrule Yam L from the Y82042 carbonaceous chondrite (in weight-%). The notations Yam A, B . . . define the area of the thinsection in which these olivines occur.

	Yam A		Yam E		Yam F	Yam G	
N	3	2	1	1	1	1	2
SiO_2	43.5	42.9	42.0	42.5	42.8	43.5	42.0
TiO_2	0.02	0.03	—	0.02	0.04	0.02	0.07
Al_2O_3	0.04	0.05	0.06	0.05	0.09	0.03	0.21
Cr_2O_3	0.42	0.45	0.40	0.40	0.52	0.44	0.19
FeO	0.86	1.15	0.74	1.44	0.74	1.01	0.68
MnO	0.11	0.16	0.07	0.12	0.09	0.11	—
NiO	0.08	—	—	—	0.07	0.05	—
MgO	55.5	54.3	56.0	55.0	55.0	55.9	56.4
CaO	0.23	0.21	0.20	0.20	0.20	0.21	0.44
Total	100.76	99.25	99.47	99.73	99.55	100.27	99.99
% Fa	0.86	1.17	0.74	1.45	0.75	1.00	0.67

	Yam J	Yam K			Yam L		Yam M
N	3	1	2	1	1	3	3
SiO_2	43.1	43.3	43.1	43.1	43.0	43.3	43.1
TiO_2	0.03	0.08	0.06	0.03	0.02	0.06	0.02
Al_2O_3	0.06	0.28	0.26	0.09	0.16	0.04	0.03
Cr_2O_3	0.41	0.09	0.15	0.12	0.19	0.31	0.17
FeO	1.17	0.53	0.66	0.52	0.76	0.83	0.73
MnO	0.07	—	0.03	0.03	—	0.09	—
NiO	—	—	—	—	—	0.03	0.04
MgO	56.0	55.8	56.3	55.8	56.0	55.8	56.2
CaO	0.30	0.50	0.44	0.33	0.44	0.33	0.03
Total	101.14	100.58	101.00	100.02	100.57	100.79	100.32
% Fa	1.16	0.53	0.65	0.52	0.76	0.83	0.72

that are moderately volatile, *e.g.,* Cr, Fe, in contrast to the data of Steele (1986a,b). The Cr_2O_3–CaO and FeO-CaO diagrams clearly show that, for the isolated olivines, there are distinct high-Ca and low-Ca olivine groups, The high-Ca group shows a negative correlation between Fe and Ca and comprises the majority of the olivines, both isolated and aggregate. For the low-Ca olivines in aggregates the data are less clear but the plots indicate a grouping similar to that of the isolated olivines.

The *isolated olivines* range in size from about 15 μm to about 250 μm in the longest dimension. They are often irregular, occasionally elongate shards and are commonly cut by veins of phyllosilicates. Frequently they are the dominant part of complex aggregates and consist typically of one large olivine surrounded by complex phyllosilicate-oxide-sulfide intergrowths, and further enveloped by fine-grained, phyllosilicate-rich material (Fig. 2). Some of these olivines contain inclusions of glass or Fe/Ni metal, or both. Their major-element compositions are nearly all highly magnesian, with less than 1.5 wt.% FeO. Excluding the rare, FeO-rich grains (*e.g.,* Yam G, Table 2), most of the minor elements in the isolated olivines display the correlations described above. In addition, the most magnesian isolated olivines show distinct high- and low-Ca groupings (Fig. 1).

Yam D is the largest, almost equidimensional isolated olivine studied (Fig. 3). It has an irregular, rounded outline and a largest dimension of 230 μm. Ca-Al glass inclusions occur in the center (Table 3), some of which contain a small bubble-like void. Closer to the rim are a few inclusions of Fe/Ni metal which range in shape from spherical to vermicular forms with the tails directed towards the rim. This metal has a fractionated Ni/Co ratio (approx. 16) and is rich in Si, Cr, and P (Table 3). Three cracks cross the Yam D olivine and are sites of some alteration. The iron and minor element concentrations of this olivine have been mapped (Fig. 4). The iron content increases from the center towards the rim and towards the cracks. Chromium also increases toward the rim. The Ca content is, as expected, at a maximum at the center of the grain, but the decrease towards the rim is not symmetrical which indicates that we are not observing simple zoning. Areas of both high-Ca and low-Ca compositions occur which cannot be explained by a monotonic change in Ca content as the crystal formed. In addition, the area richest in Al does not coincide with that of the highest Ca content (Fig. 5). Analyses of the areas of CaO and Al_2O_3 maxima (Table 4) show clear differences. These regions also differ in the distribution of Ca-Al-rich glass inclusions, all of which occur in the Ca-rich part of the crystal. In addition the distributions of Ca and Al within Yam D show another peculiarity: secondary maxima occur between the core and rim (Figs. 4 and 5). These data are shown in line scans of the isolated crystal (Fig. 6). The conventional step scan analysis indicates a hiatus between the high-Ca and low-Ca olivine compositions.

Olivines from *olivine-phyllosilicate aggregates* (Fig. 7) show compositional trends which are very similar to those of the isolated olivines (Fig. 1), with some exceptions. All olivines in aggregates are considerably smaller (10–20 μm) than the isolated olivines. This may be a result of the selection criteria, since small olivines are present outside the two main occurrences and in some cases it is not clear whether they are "isolated" or part of an aggregate. Furthermore, the compositions of the aggregate olivines do not extend to the full range of all the olivine compositions. The lowest FeO content of aggregate olivines encountered in this study was 0.52 wt.% FeO and the highest was

TABLE 2. Electron microprobe analyses of isolated olivines from Y82042 carbonaceous chondrite (in weight-%). The notations Yam A, B . . . define the area of the thinsection in which these olivines occur.

	Yam A	Yam D					
	Large	Large center Ca-rich	center Al-rich	rim 1	rim 2	rim 3	Small
N	1	4	3	4	1	2	4
SiO_2	42.9	43.0	43.1	43.0	43.4	42.2	42.8
TiO_2	0.04	0.04	0.03	—	0.02	—	0.03
Al_2O_3	0.06	0.22	0.25	0.08	0.09	0.03	0.12
Cr_2O_3	0.46	0.06	0.13	0.12	0.47	0.63	0.24
FeO	1.12	0.30	0.33	0.45	0.88	0.86	0.76
MnO	0.12	0.02	0.02	0.03	0.04	0.70	0.04
NiO	—	—	—	—	0.04	0.03	0.05
MgO	55.7	56.0	56.0	56.2	56.1	53.8	56.3
CaO	0.22	0.53	0.43	0.05	0.19	0.07	0.39
Total	100.62	100.16	100.17	99.93	101.23	98.32	100.73
% Fa	1.12	0.30	0.33	0.45	0.87	0.89	0.75

	Yam B		Yam C		Yam E	Yam G	
	Large center	rim	Small low Mn	high Mn	Small	Large low Fe	
N	1	1	2	1	2	2	main 6
SiO_2	43.4	42.0	42.7	43.0	42.8	40.7	39.3
TiO_2	—	0.02	0.04	0.03	0.05	—	—
Al_2O_3	0.07	0.07	0.18	0.09	0.10	0.04	0.06
Cr_2O_3	0.31	0.43	0.20	0.34	0.50	0.33	0.33
FeO	0.62	1.02	0.58	0.94	0.96	14.6	18.7
MnO	—	0.10	0.03	0.14	0.14	0.15	0.19
NiO	—	0.03	—	—	—	0.04	—
MgO	56.0	54.9	54.1	53.6	55.4	45.1	40.5
CaO	0.28	0.18	0.50	0.30	0.29	0.14	0.16
Total	100.68	98.75	98.33	98.44	100.24	101.10	99.24
% Fa	0.62	1.03	0.60	0.97	0.96	15.37	20.57

	Yam G	Yam I				Yam P
	high Fe	Large	Large center	rim	Small	Large
N	1	5	1	1	2	7
SiO_2	38.0	43.3	43.5	43.6	43.2	43.8
TiO_2	—	0.05	0.06	0.04	0.03	—
Al_2O_3	0.06	0.25	0.16	0.04	0.04	0.04
Cr_2O_3	0.38	0.30	0.33	0.40	0.45	0.17
FeO	22.6	0.61	0.84	0.99	2.49	0.71
MnO	0.23	0.04	0.04	0.10	0.07	0.02
NiO	0.06	—	—	0.03	—	0.03
MgO	36.7	55.5	55.4	4.6	54.0	57.4
CaO	0.19	0.35	0.28	0.33	0.32	0.02
Total	98.22	100.40	100.61	100.13	100.60	102.19
% Fa	25.68	0.61	0.84	1.01	2.52	0.69

only 1.44% in contrast to 0.26% and 22.6% FeO for isolated olivines.

Olivines from a *BO-structured object* resembling a BO chondrule (Fig. 8) are very similar in composition to the aggregate olivines (Table 1) and follow the same compositional trends. Possibly because of the small sample available of this type of olivines, no members of the low-Ca group or the high-FeO group were found.

DISCUSSION

All olivines in Y-82042 are rich in minor elements and show similar inter-element correlations. Olivines of the three principal modes of occurrence, however, differ in the range of their FeO contents. The isolated olivines show the largest compositional range, from Fa 0.25 to Fa 26. If all olivines originally formed by condensation from the solar nebula gas (the high minor element contents are in favour of such a view—see Grossman and Olsen, 1974; Olsen and Grossman, 1978; Steele, 1986a) then we can expect that the first formed olivine will be very poor in FeO (Grossman and Larimer, 1974; Palme *et al.*, 1986). Non-classical solar nebula gas compositions, considered to be more closely related to the region of chondrite formation, have been investigated (Wood and Hashimoto, 1988). The iron content of the olivine in equilibrium with one of such compositions has been calculated to be 0.25% FeO at 1400 K. This is the minimum FeO content shown by the isolated olivines, supporting our contention that these have not re-equilibrated at higher oxygen fugacities. Any larger amount of FeO now present in olivines apparently has been added at lower temperatures by a metasomatic exchange reaction (Blander and Abdel-Gawad,

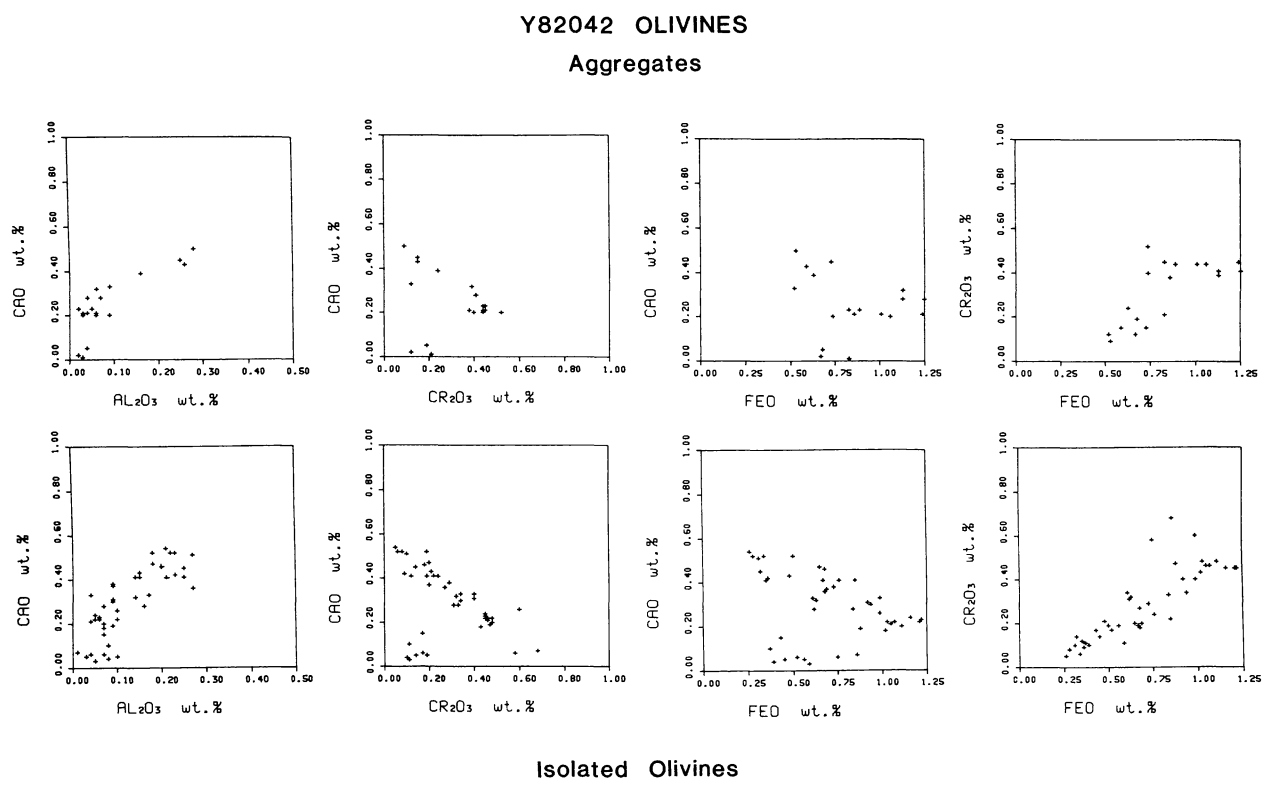

FIG. 1. Correlations of minor element contents of olivines from olivine-phyllosilicate aggregates and isolated olivines, Y-82042.

1969; Kurat, 1987, 1988; Kurat *et al.*, 1984, 1985, 1987; Peck and Wood, 1987). Whatever the presumed composition of the precursor medium, it seems clear that some of the larger isolated olivines have preserved more "primitive" compositions, *i.e.*, poorer in FeO, than the smaller olivines in aggregates (Fig. 1, Tables 1 and 2). In any case, that composition reflects more oxidizing conditions than theoretically possible during olivine condensation in a nebula of solar composition (*e.g.*, Johnson, 1986).

FIG. 2. Backscattered electron (BSE) image of two "isolated" olivine grains in Y-82042 of different composition (Fa0—dark, Fa15—gray). Both are part of aggregates consisting of complex phyllosilicate-oxide-sulfide objects in a matrix of phyllosilicates and are enveloped by fine-grained phyllosilicates (dark gray) containing a few oxide and sulphide grains. Scale bar (long dash) is 100 μm.

However, this simple model faces two major problems: (1) among the large isolated olivines there are also present the most FeO-rich compositions encountered and (2) the minor element-FeO correlations of the two olivine populations are indistinguishable. The positive correlations of the refractory elements Ca and Al can readily be explained by a co-precipitation of these elements and incorporation into the structure of the growing olivine. The co-precipitation of Ca and Al could occur from either a liquid or vapor. However, the crystal-liquid distribution coefficients do not permit the observed range in Ca contents, nor do experimental observations on the incorporation of Ca into olivine (Lofgren, 1985) produce the high Ca concen-

FIG. 3. BSE image of isolated olivine Yam D. Two metal blebs (white) are present near the upper edge of the grain. The grain and its satellite olivine are enveloped by a dense fine-grained phyllosilicate rim. Scale bar is 20 μm.

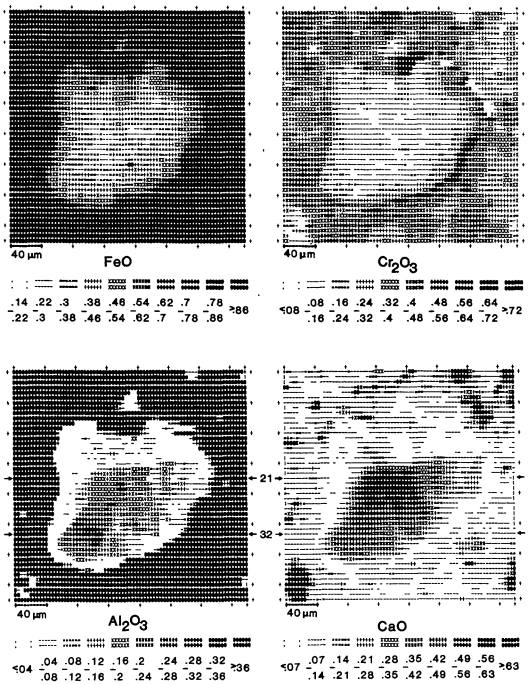

FIG. 4. Concentration maps for isolated olivine Yam D and its environs for FeO, Cr_2O_3, Al_2O_3, and CaO. FeO is very low in the central region and increases towards the rim. The high-FeO spots inside the grain mark FeNi inclusions. Cr_2O_3 is enriched asymmetrically at and outside the olivine at the right side. The Al_2O_3 maximum is off-center and the rim region is poor in Al_2O_3. The high-Al_2O_3 spots in the center mark inclusions of Ca-Al-rich glass. The CaO distribution is also asymmetric and the CaO content decreases towards the right. Arrows mark the concentration profiles across the high-Ca and high-Al regions shown in FIG. 6.

trations found in some carbonaceous chondrite olivines. Furthermore, the trends in Ca and Al contents shown by isolated olivines in Yamato 82042 are not regular and, consequently, could not have resulted from equilibrium crystallisation from a liquid. The contents of Ca and Al are also (negatively) correlated with those of the moderately volatile elements (Cr, Fe). Such correlations can be expected to result from co-condensation from a vapor rather than by crystallization from a liquid (which would produce a positive correlation) or by metasomatic exchange. This is supported by the observation that all olivines contain both refractory and moderately volatile elements in significant amounts, irrespective of their "grade of oxidation" (*e.g.*, FeO content). If, for example, Cr^{3+} had enough mobility to diffuse into the most refractory cores of large isolated olivines, why did it then not equilibrate throughout small crystals? The excellent negative correlation between Cr_2O_3 and CaO of the major compositional olivine population, for example, is incompatible with a high degree of diffusive mobility of both elements. In addition, the distribution of Ca and Al is not regular and in one olivine, Yam D, the maximum Ca content does not coincide with that of Al (Fig. 5). This new observation further supports the suggestion that solid state diffusion of cations, for example Ca and Al, has been limited. We have, therefore, to conclude that the elemental distributions observed in the olivines of Y-82042 are original and very likely due to growth from the vapor state. The observed distinction between the distribution of the Ca-rich and Al-rich areas of the olivine crystals may well result from the formation of these large olivines by the accretion of a number of much smaller crystals, each having a distinct Ca and Al distribution. These early condensing olivine grains should have complex shapes resulting from dendritic growth (*e.g.*, Brower *et al.*, 1983). Partial preservation of this could explain the complex outlines of the Ca- and Al-rich areas. Subsequently

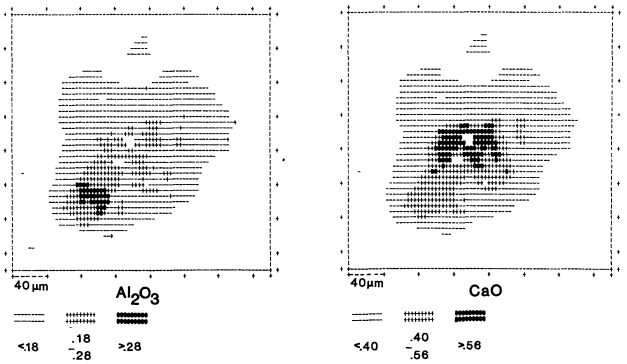

FIG. 5. Concentration maps derived from data shown in FIG. 4. showing the extent of olivine Yam D and the high, medium, and low abundance areas for Al_2O_3 and CaO. Note that the low-CaO level here is not identical with that of FIG. 4 and the low-Ca olivine group defined in this paper. The white areas inside the olivine mark the loci of glass and metal inclusions. The maxima for CaO and Al_2O_3 abundances are clearly separated. Scale as FIGS. 3 and 4.

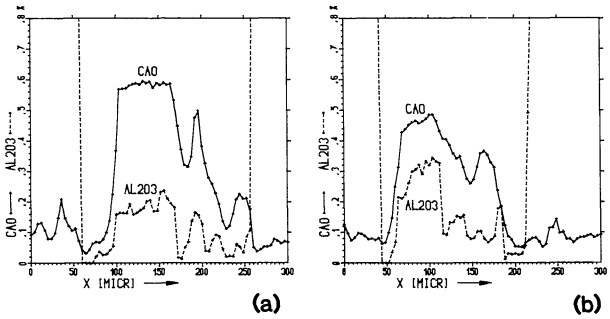

FIG. 6. Section profiles for CaO and Al_2O_3 concentrations across isolated olivine Yam D. (a) Profile through the CaO maximum (line no. 21 from to in FIG. 4, see arrows) and (b) through the Al_2O_3 maximum (line no. 32 in FIG. 4, see arrows). The crack diagonally crossing the crystal (see FIG. 3) does not affect the CaO traces but has affected the Al_2O_3 traces. These show peaks at 160 μm (trace a) and at 180 μm (trace b) caused by Al in phyllosilicates filling the crack.

TABLE 3. Electron microprobe analyses of inclusions in isolated olivines from Y82042 carbonaceous chondrite (in weight-%).

	Yam D			Yam A	
	Ca-Al-glass*	Metal		Metal	Oxide
SiO_2	44.0	Fe	85.7	90.6	50.4
TiO_2	0.55	Ni	7.7	6.3	0.54
Al_2O_3	29.4	Co	0.48	0.43	0.09
Cr_2O_3	0.11	Si	1.96	0.40	5.3
FeO	0.23	Cr	0.16	0.26	0.22
MgO	4.0	P	0.45	0.46	0.29
CaO	20.7	S	—	—	0.86
Total	98.99		96.45	98.45	57.70

* Mn, Ni, Na, K not detected.

TABLE 4. Average minor element contents (weight-%) of the high-CaO and high-Al_2O_3 classes of the isolated olivine Yam D shown in Fig. 4.

	high CaO (≥0.56)	high Al_2O_3 (≥0.28)
TiO_2	0.02	0.04
Al_2O_3	0.19	0.32
Cr_2O_3	0.11	0.13
FeO	0.32	0.36
NiO	0.02	0.04
CaO	0.59	0.46
Na_2O	0.03	0.02

condensing olivine could have filled the embayments between the early dendrites (Arrhenius and De, 1973). A later annealing event may have caused intergrowth of the early condensates which allowed a partial re-distribution of Cr and Fe while the less mobile Al was, in the main, retained in its original locations within the crystal structure.

The Ca-rich area in olivine crystal Yam D has abundant inclusions of Ca-Al-rich glass with a fairly primitive Ca/Al ratio (0.95). The composition of this glass is similar to that described from olivines in the Murchison chondrite (Fuchs *et al.*, 1973; Roedder, 1981). The glass must have been derived from a liquid which was gas-rich and which upon solidification exsolved the gas to form the abundantly present bubbles (Roedder, 1981). This liquid, however, appears not to have been in equilibrium with the host olivine. The Fe/Mg ratios and the Al_2O_3 and TiO_2 contents of the glass and olivine appear to be far out of equilibrium (Roeder and Emslie, 1970; Yurimoto and Sueno, 1984). The distribution of CaO between olivine and glass, however, apparently approaches equilibrium at high temperature (Watson, 1979). This disequilibrium distribution of several elements rules out a derivation of the olivine by crystallization from the melt, in accordance with other observations discussed above. The gas-laden liquid therefore could either have formed contemporaneously with the olivine by condensation or by exsolution from the olivine during an annealing event. The fairly primitive Ca/Al ratio of the glass could be taken as supporting a condensation origin.

A complication is that liquids cannot be expected to nucleate

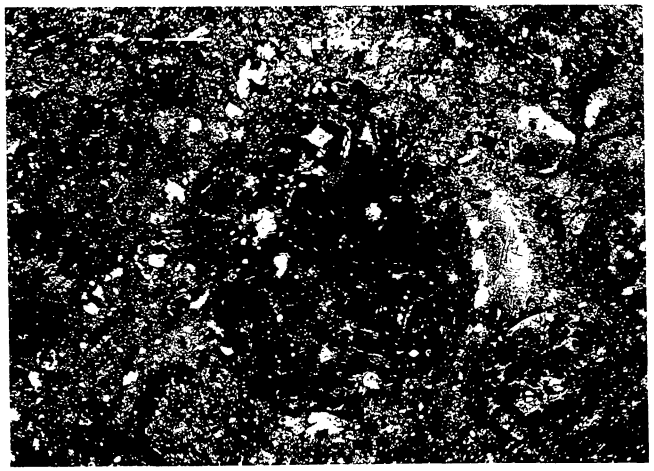

FIG. 7. BSE image of an olivine-phyllosilicate aggregate and an isolated olivine of the FeO-rich population (Fa 26; elongated grain right of the center). Scale bar (long dash) 100 μm.

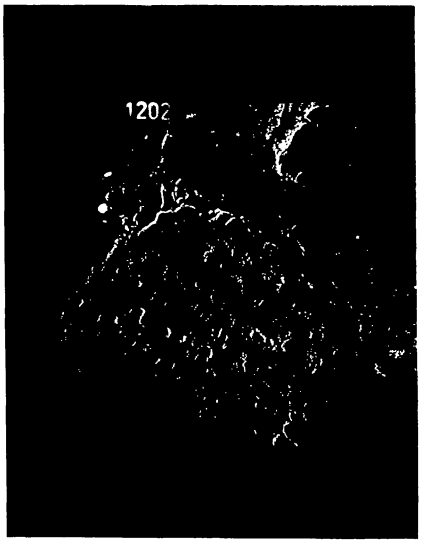

FIG. 8. BSE image of remnants of barred olivine in phyllosilicate matrix. The object is located at the edge of the thin-section and is surrounded by epoxy. Largest diameter of object is 300 μm.

and condense from a gas of solar nebula composition under the likely pressures derived from theoretical considerations (*e.g.*, Grossman and Larimer, 1974). High pressures (Grossman and Clark, 1973) or non-solar gas compositions (Wood and Hashimoto, 1988) can, however, produce liquids from the cooling gas. Thus, the presence of a liquid and its high gas content could both indicate a fairly high pressure prevailing in the region where the olivines formed.

Droplets of that liquid could have been included into the growing olivine. This olivine has a higher Ca/Al ratio than that which is not associated with the glass. It is therefore possible that the Ca-Al-rich glass marks the first oversaturation of the gas in Ca and Al, and preferentially scavenged Al relative to Ca causing lower Al contents in the contemporaneously growing olivines. These became the Ca-rich olivines. The Al-rich olivines apparently precipitated without a co-precipitating liquid. We can conclude, therefore, that the Ca-rich olivine precipitated early and included the Ca-Al-rich glass, followed by the Al-rich olivine. Subsequent olivine generations took up decreasing amounts of refractory elements and increasing amounts of moderately volatile elements.

Small metal inclusions in the olivines have compositions similar to metals reported from other chondrites and are compatible with an origin by condensation from a solar nebula gas (Grossman and Olsen, 1974; Steele, 1986a,b). The ratios of Fe/Ni and Ni/Co in the metal, however, are fractionated. They apparently indicate elevated oxygen fugacities during formation—in accordance with the relatively high FeO contents of the most magnesian olivines. In addition the partitioning of Cr between silicate and metal (Rammensee *et al.*, 1983) is also incompatible with highly reducing conditions.

CONCLUSIONS

The abundances, distributions of, and correlations among minor element contents of olivines in the Y-82042 (C2) chondrite are compatible with an origin for the crystals as solid crystalline condensates from a vapor. The first olivines to condense from

that vapor were rich in Ca and Al, contained about 0.25 wt.% FeO and apparently co-condensed with a Ca-Al-rich liquid, now represented by Ca-Al-rich glass inclusions in the Ca-rich olivines. Cessation of condensation of this liquid led to a condensation of olivines with higher Al contents and low Ca/Al ratios. Elemental distributions within large isolated olivine crystals suggest that the early olivines formed as platelets which adhered to each other in crystallographic continuity and were subsequently annealed to form a single crystal. These acted as nuclei for later condensing olivine. Smaller olivines of the olivine-phyllosilicate aggregates have higher FeO contents than the large isolated olivines but are indistinguishable in their minor element correlations from the latter. Consequently, they are interpreted as having nucleated later and grown under conditions of lower oversaturation compared to the early portions of the large isolated olivines. The almost perfect correlations among refractory and moderately volatile elements are considered to be a record of the condensation events rather than a subsequent metasomatic exchange reaction. Condensation apparently took place under non-canonical high pressure and elevated oxygen fugacities.

Acknowledgments—Financial support was provided by the Austrian "Fonds zur Förderung der wissenschaftlichen Forschung" (project P 5554, G.K., P.I.). We thank the Japanese Antarctic Meteorite Committee for providing the sample. We also thank I. Steele, J. Wood and an anonymous reviewer for helpful reviews.

Editorial handling: J. A. Wood.

REFERENCES

Arrhenius G. and De B. R. (1973) Equilibrium condensation in a solar nebula. *Meteoritics* **8,** 297–313.

Blander M. and Abdel-Gawad M. (1969) The origin of meteorites and the constrained equilibrium condensation theory. *Geochim. Cosmochim. Acta* **33,** 701–716.

Brower R. C., Kessler D. A., Koplik J. and Levine H. (1983) Geometrical approach to moving-interface dynamics. *Phys. Rev. Lett.* **51,** 1111–1114.

Desnoyers C. (1980) The Niger (I) carbonaceous chondrite and implications for the origin of aggregates and isolated olivine grains in C2 chondrites. *Earth Planet. Sci. Lett.* **47,** 223–234.

Fuchs L. H., Olsen E. and Jensen K. J. (1973) Mineralogy, mineral-chemistry and composition of the Murchison (C2) meteorite. *Smithsonian Contrib. Earth Sci.* **10,** 1–39.

Grady M. M., Graham A. L., Barber D. J., Aylmer D., Kurat G., Ntaflos T., Ott U. and Palme H. (1986) Yamato 82042: An unusual carbonaceous chondrite with CM affinities. *Mem. Natl. Inst. Polar Res. Spec. Iss.* **46,** 162–178.

Grossman L. and Clark S. P., Jr. (1973) High-temperature condensates in chondrites and the environment in which they formed. *Geochim. Cosmochim. Acta* **37,** 635–649.

Grossman L. and Larimer J. W. (1974) Early chemical history of the solar system. *Rev. Geophys.* **12,** 71–101.

Grossman L. and Olsen E. (1974) Origin of the high-temperature fraction of C2 chondrites. *Geochim. Cosmochim. Acta* **38,** 173–187.

Hoinkes G. and Kurat G. (1975) Preliminary report on the Bali carbonaceous chondrite. *Meteoritics* **10,** 416–417.

Hutchison R. and Symes R. F. (1972) Calcium variation in olivines of the Murchison and Vigarano meteorites. *Meteoritics* **7,** 23–29.

Johnson M. C. (1986) The solar nebula redox state as recorded by the most reduced chondrules of five primitive chondrites. *Geochim. Cosmochim. Acta* **50,** 1497–1502.

Koeberl C., Ntaflos T., Kurat G. and Chai C. F. (1987) Petrology and geochemistry of the Ningqiang (CV4) chondrite (abstract). *Lunar Planet. Sci.* **18,** 499–500.

Kurat G. (1975) Der kohlige Chondrit Lance: Eine petrologische Analyse der komplexen Genese eines Chondriten. *Tschermaks Min. Petr. Mitt.* **22,** 38–78.

Kurat G. (1987) The OC puzzle: Pre- and synaccretionary processes offer a solution (abstract). *Lunar Planet Sci.* **18,** 521–522.

Kurat G. (1988) Primitive meteorites: An attempt towards unification. *Phil. Trans. R. Soc. Lond.* **A 325,** 459–482.

Kurat G. and Kracher A. (1975) Preliminary report on the Cochabamba carbonaceous chondrite. *Meteoritics* **10,** 432–433.

Kurat G., Pernicka E. and Herrwerth I. (1984) Chondrules from Chainpur (LL-3): Reduced parent rocks and vapor fractionation. *Earth Planet Sci. Lett.* **68,** 43–56.

Kurat G., Palme H., Brandstätter F., Spettel B. and Perelygin V. P. (1985) Allende chondrules: Distillations, condensations, and metasomatism (abstract). *Lunar Planet Sci.* **16,** 471–472.

Kurat G., Palme H., Brandstätter F. and Huth H. (1987) Allende-AF: Undisturbed record of condensation, accretion, and metasomatism (abstract). *Lunar Planet Sci.* **18,** 523–524.

Lofgren G. E. (1985) Dynamic crystallization experiments on chondrule melts: The effects of kinetic growth factors on the chemistry of olivine and pyroxene. *Meteoritics* **20,** 699–700.

Mayr M. and Angeli J. (1985) Concentration mapping—a software package for the quantitative determination of two-dimensional elemental distributions by an electron probe microanalyzer. *X-ray Spectrom.* **114,** 89–98.

McSween H. Y. (1977) On the nature and origin of isolated olivine grains in carbonaceous chondrites. *Geochim. Cosmochim. Acta* **41,** 411–418.

Olsen E. J. and Grossman L. (1978) On the origin of isolated olivine grains in type 2 carbonaceous chondrites. *Earth Planet. Sci. Lett.* **41,** 111–127.

Palme H., Kurat G., Brandstätter F., Burghele A., Huth H., Spettel B. and Wlotzka F. (1985) An unusual chondritic fragment from the Allende meteorite (abstract). *Lunar Planet Sci.* **16,** 645–646.

Palme H., Spettel B. and Steele I. M. (1986) Trace elements in forsterite-rich inclusions in Allende (abstract). *Lunar Planet Sci.* **17,** 640–641.

Peck J. A. and Wood J. A. (1987) The origin of ferrous zoning in Allende chondrule olivines. *Geochim. Cosmochim. Acta* **51,** 1503–1510.

Rammensee W., Palme H. and Wänke H. (1983) Experimental investigation of metal-silicate partitioning of some lithophile elements (Ta, Mn, V, Cr). *Lunar Planet. Sci.* **14,** 628–629.

Roedder E. (1981) Significance of Ca-Al-rich silicate melt inclusions in olivine crystals from the Murchison type II carbonaceous chondrite. *Bull. Mineral.* **104,** 339–353.

Roeder P. L. and Emslie R. F. (1970) Olivine-liquid equilibrium. *Contr. Mineral. Petrol.* **29,** 275–289.

Skirius C., Steele I. M. and Smith J. V. (1986) Belgica-7904: A new carbonaceous chondrite from Antarctica: Minor element chemistry of olivine. *Mem. Natl Inst. Polar Res. Tokyo,* **41,** 243–258.

Steele I. M. (1986a) Compositions and textures of relic forsterite in carbonaceous and unequilibrated ordinary chondrites. *Geochim. Cosmochim. Acta* **50,** 1379–1395.

Steele I. M. (1986b) Cathodoluminiscence and minor elements in forsterite from extraterrestrial samples. *Amer. Mineral.* **71,** 966–970.

Steele I. M. and Smith J. V. (1986) Contrasting forsterite compositions for C2, C3, and UOC meteorites: Evidence for divergence from common parent (abstract). *Lunar Planet Sci.* **17,** 822–823.

Steele I. M., Cox R. T., Jr. and Smith J. V. (1984) Belgica 7904, an extreme C2 from Antarctica: Petrology and mineral chemistry (abstract). *Lunar Planet Sci.* **15,** 820–821.

Steele I. M., Smith J. V. and Skirius C. M. (1985a) Unique forsterite in chondrites. II: Compositional variation and high minor element contents (abstract). *Lunar Planet. Sci.* **16,** 817–818.

Steele I. M., Smith J. V. and Skirius C. M. (1985b) Cathodoluminescence zoning and minor elements in forsterites from the Murchison (C2) and Allende (C3) carbonaceous chondrites. *Nature* **313,** 294–297.

Watson E. B. (1979) Calcium content of forsterite coexisting with

silicate liquid in the system Na2O-CaO-MgO-A12O3-SiO2. *Amer. Mineral.* **64,** 824–829.

Wood J. A. and Hashimoto A. (1988) The condensation sequence under non-classic conditions (p < 10-3 atm, non-cosmic compositions) (abstract). *Lunar Planet. Sci.* **19,** 1292–1293.

Yurimoto H. and Sueno S. (1984) Anion and cation partitioning between olivine, plagioclase phenocrysts and the host magma: A new application of ion microprobe study. *Geochim. J.* **18,** 85–94.